Persephonella atlantica sp. nov.: How to adapt to physico-chemical gradients in high temperature hydrothermal habitats

David François, Anne Godfroy, Clémentine Mathien, Johanne Aubé, Cecile Cathalot, Francoise Lesongeur, Stephane l'Haridon, Xavier Philippon, Erwan Roussel

Persephonella atlantica sp. nov.: How to adapt to physico-chemical gradients in high temperature hydrothermal habitats

David X. François[1], Anne Godfroy[1], Clémentine Mathien[1], Johanne Aubé[1], Cécile Cathalot[2], Françoise Lesongeur[1], Stéphane L'Haridon[1], Xavier Philippon[1], Erwan G. Roussel[1] *

[1]Univ Brest, Ifremer, CNRS, Laboratoire de Microbiologie des Environnements Extrêmes UMR6197, F-29280, Plouzané, France

[2]Ifremer, Laboratoire Cycle Géochimique et Ressources (LCG/GM/REM), F-29280, Plouzané, France

* Corresponding author: Laboratoire de Microbiologie des Environnements Extrêmes, UMR6197, Univ Brest, Ifremer, CNRS, Plouzané, France. E-mail address: Erwan.Roussel@Ifremer.fr (E. Roussel).

Abstract

A novel thermophilic, microaerophilic and anaerobic, hydrogen- sulphur- and thiosulphate-oxidising bacterium, designated MO1340^T , was isolated from a deep-sea hydrothermal chimney collected from the Lucky Strike hydrothermal vent field on the Mid-Atlantic Ridge. Cells were short, motile rods of 1.4 - 2.2 µm length and 0.5 - 0.8 µm width. Optimal growth was observed for a NaCl concentration of 2.5 % (w/v) at pH 6.5. As for other members of the genus *Persephonella* , strain MO1340^T was strictly chemolithoautotrophic and could oxidise hydrogen, elemental sulphur or thiosulphate using oxygen as electron acceptor. Anaerobic nitrate reduction using hydrogen could also be performed. Each catabolic reaction had a different optimal growth temperature (65 to 75 °C) and an optimal dissolved oxygen concentration (11.4 to 119.7 µM at 70 °C for aerobic reactions) that varied according to the electron donors utilised. These experimental results are consistent with the distribution of these catabolic substrates along the temperature gradient observed in active hydrothermal systems. They strongly suggest that this adaptive strategy could confer a selective advantage for strain MO1340^T in the dynamic part of the ecosystem where hot, reduced hydrothermal fluid mixes with cold, oxygenated seawater. Phylogenetic analysis indicated that strain MO1340^T was a member of the genus *Persephonella* within the order *Hydrogenothermales* as it shared a 16S rRNA gene sequence similarity <95.5 % and ANI respectively 75.66 % with closest described *Persephonella* (*P. hydrogeniphila* 29W^T). On the basis of the physiological and genomic properties of the new isolate, the name *Persephonella atlantica* sp. nov. is proposed. The type strain is MO1340^T (=UBOCC-M-3359^T =JCM 34026^T).

Keywords

Aquificota, Persephonella, hydrothermal, chemolithoautotroph, temperature, thermophile

Introduction

Hydrothermal chimneys are mineral structures resulting from the precipitation of various chemical species during the mixing between the hot, reduced hydrothermal fluid and the cold, oxygenated seawater [31, 34]. These structures and the surrounding seawater are characterized by steep gradients: (1) chemical gradients due to the mixing of reduced compounds (e.g. H_2, CH_4, H_2S, $S_2O_3^{2-}$, Fe^{2+}) from the hydrothermal fluid, and oxidised compounds from the surrounding seawater (e.g. O_2, NO_3^-, SO_4^{2-}); and (2) thermal gradients decreasing from the inner parts of chimneys heated by hydrothermal fluid circulation (> 300 °C), to the external parts in contact with seawater (2-4 °C) [45, 51].

These gradients cause a chemical disequilibrium that supports chemoautotrophic microorganisms that oxidise reduced compounds from hydrothermal fluid using oxidised species from seawater. Hence, adaptation of these microorganisms to the thermal and chemical gradients shapes their spatial distribution across hydrothermal habitats [10, 11, 51, 74]. For example, dissolved oxygen concentrations are inversely correlated with temperature and usually separate aerobic mesophiles from anaerobic hyperthermophiles [1, 41, 45, 46]. At temperatures exceeding 80 °C, a majority of microorganisms in these environments seem to have specifically adapted to conditions that are present only at small spatial scales in the hydrothermal chimney (e.g. *Methanococcales*, *Thermococcales*) [11, 45]. However, at lower temperatures, the diversity of reactants (e.g. oxygen, nitrate, sulphides) seem to favour metabolic versatility as it was described for *Epsilonbacteraeota*, one of the dominant lineages in these habitats [5].

Members of phylum *Aquificota* are another illustration of chemoautrophic microorganisms metabolically versatile that are ubiquitous in deep-sea hydrothermal vents [18, 25, 47, 50, 58]. The phylum *Aquificota* (previously known as *Aquificae*) was first described in 2001 and contains now two classes according to the Genome Taxonomy

Database [55], *Desulfurobacteriia* and *Aquificae*. *Aquificae* are divided in two orders: *Aquificales* and *Hydrogenothermales* [14, 28, 39, 55]. All members of the phylum *Aquificota* are thermophilic or hyperthermophilic Gram-negative rods *Bacteria*, isolated from terrestrial hot ecosystems, coastal, or deep sea hydrothermal vents [29]. They share an obligate or facultative chemolithoautotrophic metabolism by fixing carbon dioxide using reductive tricarboxylic acid cycle (rTCA) [32], with hydrogen or reduced sulphur compounds as electron donors and nitrate as electron acceptors, also oxygen is used as electron acceptor by members of the class *Aquificae*. *Aquificota* mostly diverge from other phyla by displaying distinct16S rRNA gene sequences and genomic conserved signature indels [29]. Members of genus *Persephonella*, and other genera in the family *Hydrogenothermaceae* (*Hydrogenothermus, Sulfurihydrogenibium and Venenivibrio*) share the common traits described above, and show an extensive genomic diversity exhibiting a biogeographic distribution pattern [47]. Although endemic and widely distributed among deep sea hydrothermal vents the genus *Persephonella* is, to date, only composed of three described species isolated from hydrothermal vents in the Pacific ocean: *P. marina* EX-H1^T, *P. guaymasensis* EX-H2^T and *P. hydrogeniphila* 29W^T [25, 50].

In this study, we report the isolation of a novel thermophilic, microaerophilic to anaerobic, chemolithoautotrophic *Persephonella* species obtained from an Atlantic deep-sea hydrothermal vent. Characterization of this novel strain demonstrates metabolic adaptation to a wide range of physical and chemical conditions.

Material and methods

Culture, enrichment and isolation

The bottom part of the Aisics chimney (sample Chem08; 1690 m depth) [61] was sampled using the ROV *Victor 6000* during the MOMAR2008 oceanographic cruise [16] at

93 the Lucky Strike hydrothermal vent field on the Mid-Atlantic Ridge (37° 17' 20.26" N, 32°
94 16' 32.05" W). Chimney sample was brought to the sea surface in a dedicated decontaminated
95 insulated sample box. On board, chimney fragments were crushed under anoxic conditions
96 using an anaerobic chamber and stored at 4 °C in sterile serum vials filled with artificial
97 sterile seawater (Sea salts, Sigma Aldrich) under a N_2 atmosphere. Ten years later, 0.5 mL of
98 hydrothermal chimney slurry was used to inoculate the medium described below. X-ray
99 diffraction analysis showed that chimney sample was mainly composed of sulphides including
100 chalcopyrite, pyrite and marcasite (Ewan Pelleter, personal communication).
101 Enrichment cultures were performed in 50 mL glass bottles sealed with butyl septa,
102 and containing 20 mL of the medium described by Parkes *et al.* omitting Na_2S and $FeCl_2$
103 solutions [54]. This medium contained per litter: NaCl (24.3 g), $MgCl_2.6H_2O$ (10 g),
104 $CaCl_2.2H_2O$ (1.5 g), KCl (0.66 g). Trace elements were provided by SL-10 solution (1 mL),
105 Selenite-Wolfram solution (0.2 mL), and 1 mL of KBr (0.84 M), H_3BO_3 (0.4 M), $SrCl_2$ (0.15
106 M), NH_4Cl (0.4 M), KH_2PO_4 (0.04 M) and NaF (0.07 M) solutions. The medium was
107 sterilized by autoclaving for 30 minutes at 100 °C and was buffered by adding $NaHCO_3$ (2.52
108 g).
109 Thiosulphate was added at a final concentration of 10 mM as electron donor. Gas phase was
110 composed of N_2:CO_2 (80:20, 150 kPa) and 1 mL of sterile air was added with a syringe in
111 order to create microaerophilic conditions. After 12 days incubation at 30 °C without
112 agitation, subcultures from positive enrichment were consecutively incubated 7 days at 50 °C
113 and 7 days at 60 °C. Strain MO1340^T was isolated by three consecutive tenfold dilutions in
114 Hungate anaerobic tubes incubated at 60 °C in the same medium as for the enrichment step.
115 Five successive transfers were also performed on medium solidified with 1 % gellan gum
116 (Sigma Aldrich) incubated at 70 °C in serum vials with hydrogen as energy source (gas phase

117 H_2:CO_2 80:20, 200 kPa) and nitrate as electron acceptor (8 mM). Purity of the strain was
118 regularly checked by microscope observation and 16S rRNA gene sequencing.
119 *Morphological characterization*
120 Cells morphology and motility of strain MO1340^T were observed under an Olympus
121 BX60 phase contrast microscope. Transmission electron microscopy observations were
122 performed without staining on exponential phase cultures grown on thiosulphate and oxygen
123 at 70 °C (JEM-1400, JEOL; *Plateforme d'Imagerie et de Mesures en Microscopie*, University
124 of Brest).
125 *Physiology and growth requirements*
126 Unless otherwise stated, all physiological characterizations were done in anaerobic
127 Bellco tubes (Bellco Glass Inc., Vineland N.J.) in triplicate filled with 15 mL of the medium
128 described above at pH 6.8, incubated without agitation at 70 °C. Uninoculated media blanks
129 were used as negative controls for each culture condition. Growth was determined from cell
130 counting by microscope observation using Thoma cell counting chamber (depth: 0.02 mm).
131 Flow cytometry counting was also performed on cells fixed with 2.5 % (w/v) glutaraldehyde
132 and stored at 4 °C. Cell samples were diluted 10 to 100 times in a saline solution with 2.5 %
133 (w/v) NaCl and stained with SYBRGreen I (Sigma Aldrich). Cells were counted using a
134 Cyflox Space (Sysmex, Partec).
135 Dissolved oxygen requirement was determined by increasing oxygen concentration in
136 the gas phase from 0 to 21 % at 150 kPa (0 to 179.5 µM of dissolved oxygen) in 3 different
137 media containing respectively (1) thiosulphate (10 mM); (2) colloidal elemental sulphur 1 %
138 (w/v); or (3) hydrogen (80 % in the gas phase, 200 kPa; 820.7 µM of dissolved hydrogen) as
139 electron donors. The influence of temperature on growth was determined for temperatures
140 ranging from 40 to 85 °C in 4 different culture conditions: in the presence of (1) thiosulphate
141 (10 mM) under N_2:CO_2:O_2 gas phase (77.5:20:2.5, 150 kPa; 21.4 µM of dissolved oxygen);

(2) elemental sulphur (1 %, w/v), under N_2:CO_2:O_2 gas phase (66:20:14, 150 kPa; 119.7 µM of dissolved oxygen); (3) hydrogen in anoxic conditions with nitrate (8 mM) as electron acceptor under H_2:CO_2 gas phase (80:20, 200 kPa; 820.7 µM of dissolved hydrogen); and (4) hydrogen in microaerophilic conditions under H_2:CO_2:O_2 gas phase (79:20:1, 200 kPa; 820.7 µM of dissolved hydrogen; 11.4 µM of dissolved oxygen). NaCl concentration and pH optimum and range were determined on thiosulphate (10 mM) containing medium, under N_2:CO_2:O_2 (77.5:20:2.5, 150 kPa) gas phase. NaCl concentrations tested ranged from 0 to 5.5 % (w/v). pH was adjusted from 4.5 to 6 by adding increasing volumes of sterile solutions of 1% (w/v) $NaHCO_3$ to medium without buffer. For pH above 6, 2 % (w/v) Na_2CO_3 was added to medium buffered with 2 mM $NaHCO_3$ (instead of 30 mM in standard medium).

Electron donor and acceptor requirement

Electron donors were tested by supplementing mineral medium (artificial seawater described above, without Na_2S nor $FeCl_2$) with: hydrogen (80 % in the gas phase, 200 kPa), formate (10 mM), succinate (10 mM), ferrous iron (10 mM), acetate (1 mM), ammonium chloride (15 mM) or elemental sulphur (1 % w/v). Oxygen (1.5 or 7 % in the gas phase, 150 kPa) or nitrate (10 mM) were added as electron acceptors in all conditions. The following electron acceptors were tested in presence of H_2:CO_2 (80:20, 200 kPa): sulphate (10 mM), sulphite (10 mM), nitrite (1 or 14 mM), ferric iron (10 mM), elemental sulphur (1 % w/v), acetate (1 mM) or thiosulphate (10 mM). Organic carbon sources were tested in presence of N_2:CO_2:O_2 (73:20:7, 150 kPa) at a final concentration of 2 g/L (yeast extract or peptone) or 5 g/L (glucose, sucrose, fructose, lactose or sorbitol). Mixotrophic growth was tested using yeast extract (0.5 g/L), peptone (0.5 g/L) and glucose (1 g/L) as carbon sources and sodium bicarbonate was replaced by PIPES disodium salt (6 g/L). Hydrogen (200 kPa) and nitrate (10 mM), or thiosulphate (10 mM) or sulphur (1 % w/v) in the presence of oxygen (7 % in the gas phase, 150 kPa) were provided as energy sources.

Consecutive positive cultures were transferred three times on the same medium to ensure that growth was not due to substrate carry-over from the inoculum. Controls containing no electron acceptor or donor were performed. Utilisation of various electron donors and acceptors were also performed on the closest relative to strain MO1340^T, *Persephonella hydrogeniphila* 29W^T (DSM 15103) provided by the German Collection of Microorganisms and Cell Cultures. Growth in the absence of Balch vitamins solution was tested (as recommended in [71]) using the standard medium in the presence of thiosulphate and oxygen. In order to identify the metabolic reactions performed by strain MO1340, end-point cultures were carried out and both substrates consumption and metabolic by-products were quantified. Four couples of substrates were tested ($S_2O_3^{2-}/O_2$; S^0/O_2; H_2/O_2; H_2/NO_3^-) in the same conditions as described above. At least three negative controls and 3 to 10 culture replicates were performed and incubated at 70 C.

Analytical techniques

Hydrogen, nitrogen and carbon dioxide concentration in the headspace phase were measured using a modified INFICON/Micro GC FUSION Gas Analyser (INFICON, Basel, Switzerland) fitted with a pressure gauge (CTE8005AY0, Sensortechnics GmbH) and two conductivity detectors. Separation was performed using two columns: molecular sieve 10m column and argon as a carrier gas; and a RT-Q 12m using helium as a carrier gas. Gas concentrations were calculated using the method of Mah *et al.* [42]. Concentrations of dissolved oxygen and hydrogen in the experimental conditions were calculated for seawater at 70 °C as described respectively by Weiss *et al.* [81] and Crozier *et al*. [9].

Thiosulphate, nitrate and sulphate concentrations were quantified by anion chromatography using a Dionex ICS-2000 Reagent-Free Ion Chromatography System (Thermo Fisher Scientific) as described by Webster *et al*. [80]. A potential hydrogen peroxide production was assayed by using the MyQubit Amplex^{TM} Red Peroxyde Assay (Invitrogen)

192 according to the manufacturer's recommendation. Stoichiometry of the reactions were
193 calculated from experimental data and then compared to metabolic reactions described in
194 literature [2, 78].
195 *Thermodynamic calculations and Arrhenius parameters*
196 To quantify the energy gained from each reactional pathway considered, we calculated the
197 overall Gibbs free energy of the reaction derived from the following expression (Eq. 1)
198 $\Delta_r G = \Delta_r G_0 + RTlnQ_r$ Eq.1
199 Where $\Delta_r G_o$ represents the standard state Gibbs free energy of reaction, R is the gas constant,
200 T is temperature in Kelvins and Q_r stands for the activity product for the natural conditions.
201 The activity product Q_r is given by Eq.2
202 $Q_r = \prod a_i^{\gamma_{i,r}}$ Eq. 2
203 Where a_i stands for the activity of the i^{th} constituent of the reaction r, and $\gamma_{i,r}$ represents the
204 stoichiometric reaction coefficient (negative for reactants, positive for products). Activities
205 are derived from concentrations through the extended Debye-Huckel equation for activity
206 coefficients. Thermodynamic and hydrodynamic modelling were performed on R [77] using
207 the CHNOSZ database [12] and ReacTran [69], gsw [37] and marelac [70] packages. The
208 metabolic pathways and reactions considered in this work are listed in Table 2.
209 Concentrations of the chemical species at various temperatures were determined following
210 two approaches. 1) When available, we used *in situ* data collected along the mixing gradient
211 between end member hydrothermal fluid at Aisics chimney and surrounding seawater using
212 the PEPITO water sampler [8], coupled to an oxygen Aanderaa optode and the CHEMINI *in*
213 *situ* chemical analyser for total sulphide concentrations [79]. 2) When not available, a simple
214 hydrodynamic model was used to predict dilution processes along the mixing gradient and
215 calculate concentrations assuming simple mixing (i.e. no reaction) between the hydrothermal
216 fluid and the surrounding seawater. Values of the end-member fluid are based on the literature

[6, 61] or inferred from other hydrothermal sites when no data are available on Aisics ([19] for elemental sulphur). *In situ* data were collected during the MOMARSAT 2015 cruise on board R/V Pourquoi Pas? [65]. Fluid samples were analysed back on shore for nitrate, sulphate and thiosulphate concentrations using anion chromatography as described by Webster *et al*. [80].

Concentrations of the end-member fluid might have changed since the strain was initially collected in 2008. However reported concentrations of Aisics high temperature fluids show limited variability [6, 61] and we therefore expect only minor alteration of the distribution of chemical species along the mixing gradient over the years.

The effect of temperature on specific growth rate was studied using Arrhenius plots and Q_{10} values that were calculated as described by Roussel *et al*. 2015 [62]. Statistical analysis and multiple peek fitting were performed using Origin 2016 (OriginLab Corporation, Northampton, USA) with the multiple peak fit tool using the Gauss peak function.

Genome sequencing and analysis

Genomic DNA of strain MO1340^T was isolated by PCI extraction [82] from cells grown on thiosulphate and oxygen at 70 °C. 16S rRNA gene was amplified by PCR using bacterial primers E8F and U1492R [13]. The gene was sequenced in triplicate using Sanger technology (Eurofins, Germany). Gene sequence (1444 bp) was deposited in the GenBank/EMBL/DDBJ databases under accession number MT376293.

The 16S rRNA sequences from strain MO1340^T and 11 of the closest *Hydrogenothermales* obtained by BLASTN search were then edited (1364 bases) in the Geneious v10.2.3 program and aligned using MUSCLE program [15, 36]. Phylogenetic reconstructions were made on the basis of evolutionary distance using neighbour-joining [63] and maximum-likelihood methods with Tamura-Nei correction (respectively modelled with G

241 and G+I parameters) using the MEGA 7 software [38, 75]. The reliability of internal branches
242 was assessed using the bootstrap method with 1000 replicates [17].
243 Genome sequence determination of strain MO1340^T was carried out using Illumina
244 HiSeq technology (Eurofins Scientific, Germany). Genome assembly was performed using
245 spades v.3.13.0 ([3]). Completion and contamination were assessed using CheckM [56] and
246 quality of the genome sequence was checked using the Quality Assessment Tool for Genome
247 Assemblies (QUAST) [30]. Genome was annotated using PGAP (Prokaryotic Genome
248 Annotation Pipeline) [76]. Average Nucleotide Identity (ANI) values were calculated with the
249 OrthoANIu algorithm [87] and can accurately replace DNA–DNA hybridization values for
250 strains for which genome sequences are available [24].
251
252 **Results and discussion**
253 *Morphology and physiology of strain MO1340^T*
254 Strain MO1340^T morphological, physiological, genomic and metabolic features and
255 those of its closest relatives within the phylum *Aquificota*, family *Hydrogenothermaceae* are
256 presented in Table 1. Cells of strain MO1340^T were Gram-negative short rods from 1.4 - 2.2
257 (SD=0.42 µm, n = 33) µm length and from 0.5 - 0.8 µm width (SD=0.13 µm, n = 33), and
258 were in the range of cell sizes reported for the other *Persephonella* species (Table 1). Irregular
259 cocci were frequently observed at temperatures close to the limits for growth. TEM
260 observation showed that one-third of the cells had a single polar flagellum (Fig. 1). However,
261 motility was rarely observed, in most cases for dividing cells and in medium containing
262 elemental sulphur. On solid media, round and orange colonies (1 mm in diameter) were
263 observed after 1 to 3 days whereas cultures in liquid media were colourless.
264 Growth was observed for strain MO1340^T at NaCl concentrations ranging from 1.5 to
265 3.5 % (w/v) with an optimum at 2.5 % and at pH between 5.3 and 7.0 with an optimum

around 6.5, suggesting these microorganisms are mostly adapted to habitats where the hydrothermal fluid mixes with the seawater. Although strain MO1340^T was characterized for these parameters in presence of thiosulphate and dioxygen, optimal NaCl concentration and pH for growth were similar to those obtained for all of *Persephonella* species grown with hydrogen and nitrate (i.e. NaCl : 2.5% ; pH : 6.0 to 7.2; Table 1). However, as detailed in the last section "*Physiological and metabolic adaptation to a contrasted environment",* the optimal growth temperature (i.e. 65 to 75 °C) and dioxygen dissolved concentration (i.e. 11.4 to 119.7 µM) were substrate-dependent.

Insights into the metabolism of Persephonella *strain MO1340^T*

Like other *Persephonella* isolates, strain MO1340^T was able to grow chemolithoautotrophically on various inorganic catabolic substrates. This includes oxidation of reduced-sulphur compounds, hydrogen-oxidation, aerobic respiration or nitrate-reduction [25, 50]. The isolate grew in microaerphilic conditions with thiosulphate (10 mM), elemental sulphur (1 % w/v) or hydrogen (dissolved concentration 820.7 µM). Interestingly, the optimal oxygen concentrations varied according to electron donor and acceptor (optimum dissolved concentrations from 11.4 to 119.7 µM at 70 °C). Strain MO1340^T was also able to grow anaerobically with hydrogen as electron donor (dissolved concentration 820.7 µM) using nitrate (8 mM) as final electron acceptor. In order to compare strain MO1340^T to its closest relative, growth requirements were also tested in the same conditions using *P. hydrogeniphila* 29W^T (DSM 15103). Although *P. hydrogeniphila* 29W^T was initially described as only capable of using hydrogen as electron donor [50], growth kinetic showed it could also oxidise thiosulphate to sulphate with oxygen as electron acceptor (Fig. SM 1, Table 2), which is congruent with the presence in its genome of core genes *soxABXYZ* (GenBank accession number: PRJEB22457). Moreover, no aerobic or anaerobic growth was observed for

291 *Persephonella* strain *MO1340^T* in the presence of all tested organic carbon sources (yeast
292 extract, peptone, glucose, sucrose, fructose, lactose, or sorbitol) even in presence of carbon
293 dioxide. In the absence of vitamins, growth was not inhibited, even after five subcultures,
294 showing strain MO1340^T is a strict autotroph using only carbon dioxide as sole carbon source
295 as defined by Srinivasan *et al.* [71].
296 Substrates consumption and metabolites production by strain MO1340^T were
297 measured in order to establish stoichiometry of each catabolic reaction and infer the
298 associated standard Gibbs energy. Measured stoichiometry were consistent with the reactions
299 described by Amend *et al.* [2] (Table 2), excepted for aerobic elemental sulphur oxidation
300 where discrepancies were observed. We hypothesize that it might result from unquantified
301 intracellular metabolic intermediates accumulation. For anaerobic hydrogen-depended
302 denitrification, strain MO1340^T realised a complete reduction of nitrate to nitrogen without
303 accumulation of nitrite, nitrous oxide or ammonium which is consistent with previous studies
304 on *P. hydrogeniphila* 29W^T [50]. Moreover, in order to accurately determine the reaction
305 involved in aerobic hydrogen oxidation, as the end-product of aerobic hydrogen oxidation can
306 either be water ($2\ H_2 + O_2 \rightarrow 2\ H_2O$) or hydrogen peroxide ($H_2 + O_2 \rightarrow H_2O_2$) [78], hydrogen
307 peroxide production was assessed. As no production of hydrogen peroxide was detected,
308 strain MO1340^T can probably perform the Knallgas reaction as commonly described for other
309 *Aquificota* [27, 28]. Thermodynamic calculations based on the geochemical conditions
310 measured *in situ* at Lucky Strike vent field showed that energy provided by this reaction could
311 reach - 280 kJ/mol (Table 2), suggesting aerobic hydrogen oxidation could be a significant
312 metabolism in hydrothermal ecosystems [44, 66].
313 *Physiological and metabolic adaptation to a contrasted environment*
314 Growth rate measurements showed that strain MO1340^T exhibited different responses
315 to temperature depending on the catabolic reactions involved. Optimal growth temperatures

were respectively 65, 70, 70-75 and 75 °C for the following redox couples: S^0/O_2, $S_2O_3^{2-}/O_2$, H_2/O_2, H_2/NO_3^-. All curves for the determination of optimal growth temperature presented a plateau between 5 and 15 °C below the optimal growth temperature (Fig. 2). This curve shape was also previously observed for *P. hydrogeniphila* $29W^T$ (supplementary data in ref. [50]) that is the closest relative of strain $MO1340^T$. Arrhenius plots obtained from data of optimal growth temperature experiments on strain $MO1340^T$ also revealed two distinct slopes at sub-optimum temperatures separated by a "critical temperature" instead of a single linear slope (Fig. SM 2). Various microorganisms exhibiting growth that does not meet the square root equation [57] have also been described in studies of mesophilic and thermophilic and psychrophilic *Bacteria* [26, 48, 53]. Wiegel *et al*. suggested that these broken Arrhenius plots could be the consequence of the expression of different sets of key enzymes capable of undergoing conformational changes at different temperatures [83-85]. Moreover, the effect of temperature on the specific growth rate fitted different bimodal Gaussian patterns (R^2 = 0.96 to 1) depending on the catabolic pathway (Fig. 2). Each bimodal pair could be grouped according to the composition of the electron donor involved (i.e. sulphur or hydrogen; Fig. 2). For sulphur based electron donors (i.e. elemental sulphur and thiosulphate) both peaks were comprised between 52.7 - 56.3 and 67.4 - 68.8 °C, whereas for hydrogen both peaks were comprised between 59.8 - 63.7 and 74.1 - 74.2 (table 2 and Fig. 2), suggesting that the ≈7 °C shift depending on the electron donor could be the consequence of a different temperature range for the enzymes involved in each catabolic pathways (Sox enzymes or hydrogenases). For example, it was shown for *Hydrogenobacter thermophilus,* another member of phylum *Aquificota*, but in the order *Aquificales*, which presents physiological characteristics close to those of strain $MO1340^T$ [35], that the Sox enzymes implied in aerobic thiosulphate oxidation exhibited an optimal activity at lower temperature than the nitrite reductase (respectively 60 and 70 - 75 °C) [64, 73].

Oxygen requirements of strain MO1340^T also depended on the electron donor used. The optimal dissolved oxygen concentration was 11.4 µM (0.7 mM in gas phase) for hydrogen oxidation, and was comparable to other *Persephonella* species (0.73 to 1.21 mM in gas phase) in the same culture conditions [25, 50]. However this value was 5 to 11 fold higher in the presence of thiosulphate or elemental sulphur, respectively 59.8 and 119.7 µM (3.68 and 7.36 mM in gas phase). Comparison of growth parameters of each catabolic reaction performed by strain MO1340^T showed that optimal growth temperature and optimal oxygen concentration were inversely correlated (table 2 and Fig. 3). For example, oxidation of sulphur species such as thiosulphate and elemental sulphur allowed growth at higher oxygen concentration and at lower temperature (respectively 59.8 and 119.7 µM dissolved oxygen and 65/70 °C) whereas hydrogen oxidation coupled to oxygen reduction was optimal with only 11.4 µM oxygen at 70-75 °C. Anaerobic hydrogen oxidation coupled to nitrate reduction was optimal at a higher temperature (75 °C) compared to microaerophilic metabolisms. This inverse relationship between temperature and oxygen concentration was congruent with the geochemical gradients observed *in situ* where oxygen depletion occurs as temperature increases along the mixing gradient between the cold deep seawater and the hot hydrothermal fluid that is expelled at the seafloor (Fig. 3).

In order to estimate the energy provided by catabolic reactions performed by strain MO1340^T in natural settings, thermodynamic calculations were taken into consideration. We used *in situ* data collected along the mixing between seawater and the hydrothermal fluid from Lucky Strike, the site from which the strain was isolated. When data were not available, we used a numerical model to predict dilution of the substrates considered along the mixing gradient. The observed and predicted thermal and chemical gradients in the mixing zone were used as proxies to determine the geochemical settings of hydrothermal chimneys, in order to calculate the Gibbs free energy under *in situ* conditions (ΔGr) for each catabolic reaction of

366 strain MO1340^T at its optimal temperature (Table 2). Elemental sulphur and thiosulphate
367 oxidation reactions were the most energetic (respectively -517 and -731 kJ/mol) compared to
368 aerobic and anaerobic hydrogen oxidation reactions (respectively - 280 and - 271 kJ/mol).
369 Comparison of the ΔGr values over a large temperature range from 5 to 153 °C (Fig. SM 3)
370 showed that energy gained from elemental sulphur and thiosulphate oxidation decreased as
371 the temperature increased due to oxygen depletion, in contrast to aerobic and anaerobic
372 hydrogen oxidation, which was more energetic at higher temperature. This is consistent with
373 optimal temperature measurements of strain MO1340^T that showed a faster growth for
374 oxidation of sulphur compounds at lower temperature than for aerobic and anaerobic
375 hydrogen oxidation. Moreover, for aerobic hydrogen oxidation, the optimal ΔGr value was
376 reached at temperature above 72 °C (-280 kJ/mol, Fig. SM 3), which was congruent with the
377 experimental results on strain MO1340^T that presented an optimal growth temperature at 70-
378 75 °C when grown on these substrates. However, the calculated Gibbs free energies in *in situ*
379 conditions do not fully explain this phenomenon but rather provide tendencies. Several
380 reasons may explain slight discrepancies. First, the temperatures and substrate concentrations
381 used in the ΔG_r calculations are predicted from the mixing gradient between the end-member
382 hydrothermal fluid expulsed at the seafloor and the surrounding seawater, i.e. within an open
383 media. This might not exactly reproduce the conditions prevailing in a hydrothermal chimney,
384 where chemical and thermal gradient are squeezed due to the structure and porosity of the
385 chimneys [11]. For species derived from the simple dilution model (elemental sulphur,
386 hydrogen and nitrogen), biotic and abiotic reactions may occur early along the mixing
387 gradient including precipitation and solubilisation processes further altering the distribution of
388 electron donors and acceptors along dilution [40]. However, good convergence between
389 theoretical and *in situ* sulphate distribution (Fig. SM 4) gives us confidence that model
390 outputs are sufficient to set a reliable baseline for thermodynamic calculations. More complex

391 thermodynamic modelling including anabolic and dissipation energy requirements and effect
392 of substrate availability would be necessary to fully resolve microbial growth rates close to
393 incubation observations.

394 The physical and chemical conditions along the hydrothermal gradient shape the
395 taxonomic and functional distribution of microbial communities in hydrothermal vents [41,
396 45, 46]. For example, aerobic mesophiles are frequently observed in the periphery of
397 chimneys whereas anaerobic hyperthermophiles are present in inner parts [10, 74], with some
398 exceptions depending on the structure and porosity of chimneys [52]. Unlike strict aerobes or
399 anaerobes that could only colonize specific microhabitats in hydrothermal chimneys,
400 metabolically versatile *Aquificota* strain MO1340^{T} could settle in contrasted parts of
401 chimneys due to its ability to use different electron acceptors (i.e. oxygen or nitrate). This
402 capacity to colonize numerous microhabitats in hydrothermal ecosystems was confirmed by
403 microbial diversity analysis using high-throughput sequencing that showed the presence of
404 phylotypes related to strain MO1340 in chimneys and associated fluids from the gradient at
405 five sites of the Lucky Strike vent field (unpublished results). As for *Aquificota,*
406 *Campylobacterota* (previously included in the former phylum *Epsilonbacteraeota*) also
407 exhibit similar catabolisms such as oxidation of reduced sulphur compounds and hydrogen
408 with both oxygen and nitrate [5]. Hence, these versatile chemolithoautotrophic microbial
409 communities thrive in a wide range of habitats along the hydrothermal gradient and therefore
410 probably drive a significant fraction of the primary production at deep-sea hydrothermal
411 systems [5, 49, 60, 68]. Moreover, it has also been suggested that a specific distribution
412 within these different taxonomic groups could also occur along the hydrothermal fluid
413 gradient. For example, within *Campylobacterota, Campylobacterales* seem to thrive at lower
414 temperatures (i.e. from 20 °C to 40 °C) whereas *Nautiliales* could colonise habitats between
415 40 °C to 60 °C [5, 20]. *Aquificota* could dominate niches exceeding 60 °C as they also show a

wide catabolic and temperature adaptation that follows the hydrothermal gradient as for strain MO1340^T. This metabolic versatility and their broad temperature range could therefore provide an ecological advantage in colonizing such a dynamic part of the ecosystem compared to other chemoautotrophic microorganisms (Fig. 3). More comprehensive studies should be conducted using combination of physiological, genomic, and ecological approaches focusing this strain and others members of phylum *Aquificota* and *Epsilonbacteraeota*.

Genomic features and phylogenetic position

The draft genome of strain MO1340^T (5 contigs > 500 bp, coverage 840 x) has been deposited in GenBank/EMBL/DDBJ under the accession number JAACYA000000000. The genome characteristics such as size (1.892.283 bp, 99.59 % completion, 1.68 % contamination) average DNA G + C content (37.07 mol%) and number of coding sequences (2028 CDS) were comparable with those of previously sequenced genomes of *Persephonella* strains (Table 1). ANI values with *P. hydrogeniphila* 29W^T and *P. marina* EX-H1^T (respectively 75.66 % and 72.97 %) were well below the threshold (95-96 %) for differentiating species [7].

Analysis of draft genome of strain MO1340^T also provided details on the metabolic pathways involved in sulphur and hydrogen oxidation, nitrogen and oxygen reduction, and in carbon fixation. Thiosulphate oxidation may be performed by the sox pathway [21, 22] as all core genes *soxABXYZ* were present, excepted for *soxCD* genes that were not detected. Although it was shown that organisms that lack *soxCD* genes are often unable to completely oxidise thiosulphate to sulphate [23, 67], strain MO1340^T produced sulphate in stoichiometric quantities to the amount of thiosulphate added, suggesting an alternative pathway that could complete oxidation to sulphate. Numerous genes encoding hydrogenases were also detected, including [Ni-Fe]-Hydrogenases-genes, which is consistent with the ability of the strain to oxidise hydrogen. More than 30 genes encoding for cytochromes (bc, c, c1, c3, cbb3 and d -

type) were detected and were probably specific to the strain microaerophilic lifestyle. In anaerobic conditions, a complete reduction of nitrate was achieved as genes encoding nitrate reductase (NapAGH), nitrite reductase (NirS), nitrite oxide reductase (Nor) and nitrous oxide reductase (NosZD) were present. Autotrophic carbon dioxide fixation is performed using the "A-type" reductive tricarboxylic acid (rTCA) cycle, like others members of genus *Persephonella* and family *Hydrogenothermaceae* [32, 59]. As for the Calvin-Benson-Bassham cycle, the rTCA cycle is one of the dominant carbon fixation pathways in hydrothermal vents [33, 43], although it seems more adapted to high-temperature and low oxygen environments, which is congruent with the physiology of strain MO1340^T [4, 33, 49].

In dynamic hydrothermal ecosystems, the flagella-mediated motility and chemotaxis are essential for microorganisms to respond to variation of environmental conditions (e.g. pH, temperature) and to find substrates for growth (for e.g. [86]). Microscopic observations showed motile cells were mainly observed in medium containing elemental sulphur, suggesting a close relationship between flagella and sulphur-oxidizing systems as previously observed for *Acidithiobacillus* spp. [86]. This link was confirmed by the presence in the genome of strain MO1340^T of several genes implied in motility or chemotaxis (*FlgGAHIJBC*, *FlhAFB*, *FliGMNEFR*) that clustered with genes encoding transcriptional regulators, such as sigma factors, or genes responsible for chemotaxis (*CheZ*, *CheA*, *CheW* and *CheV*). Regulation of motility and chemotaxis by sulphur may therefore also contribute to surface colonisation of microniches in hydrothermal chimneys.

Based on phylogenetic analyses of the 16 rRNA gene sequence (Fig. 4), strain MO1340^T belongs to the genus *Persephonella* , family *Hydrogenothermaceae* order *Hydrogenothermales*. The closest described species are *P. hydrogeniphila* 29W^T, *P. marina* EX-H1^T and *P. guaymasensis* EX-H2^T with respectively 95.5 %, 93.8 % and 94.0 % 16S rRNA gene sequence similarity. These values are below the previously published cut-off

threshold of 98.7 % for species delineation, which is congruent with ANI values to other species in the genus [7]. AAI values to other Persephonella spp. fell into the range of interspecies AAI values confirming its novelty in the genus. On the basis of its physiological, metabolic and genomic characteristics, we propose that strain MO1340^T (=UBOCC-M-3359 = JCM 34026) represents a novel species within the genus *Persephonella*, for which we suggest the name *Persephonella atlantica* sp. nov, as a reference for being isolated from a hydrothermal vent field on the Mid-Atlantic Ridge.

Acknowledgements

The authors also thank the crew of the R/V *L'Atalante* and R/V *Pourquoi pas ?* and pilots of the ROV Victor 6000 for assistance in collecting samples. We thank Philippe Elies from the Plateforme d'Imagerie et de Mesures en Microscopie (PIMM), University of Brest for the transmission electron microscopy pictures. This work was supported by the ABYSS project with Ifremer.

Authors contribution

David François: Investigation, Writing - Original Draft. **Anne Godfroy**: Supervision, Samples collection. **Clémentine Mathien**: Investigation. **Johanne Aubé**: Genome assembly. **Cécile Cathalot**: Thermodynamic modelling. **Françoise Lesongeur**: Samples collection. **Stéphane l'Haridon**: Investigation, Methodology. **Xavier Philippon**: Investigation. **Erwan Roussel**: Conceptualization, Investigation. All authors: Writing - Review

Figure legends

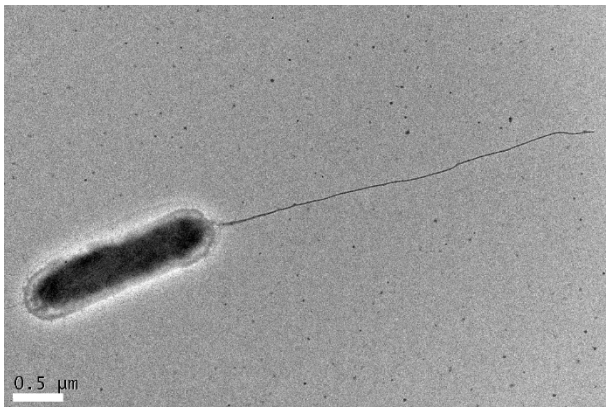

Figure 1. Transmission electron micrograph of a cell of *Persephonella atlantica* strain MO1340^T showing the polar flagellum. Scale bar represents 0.5 µm.

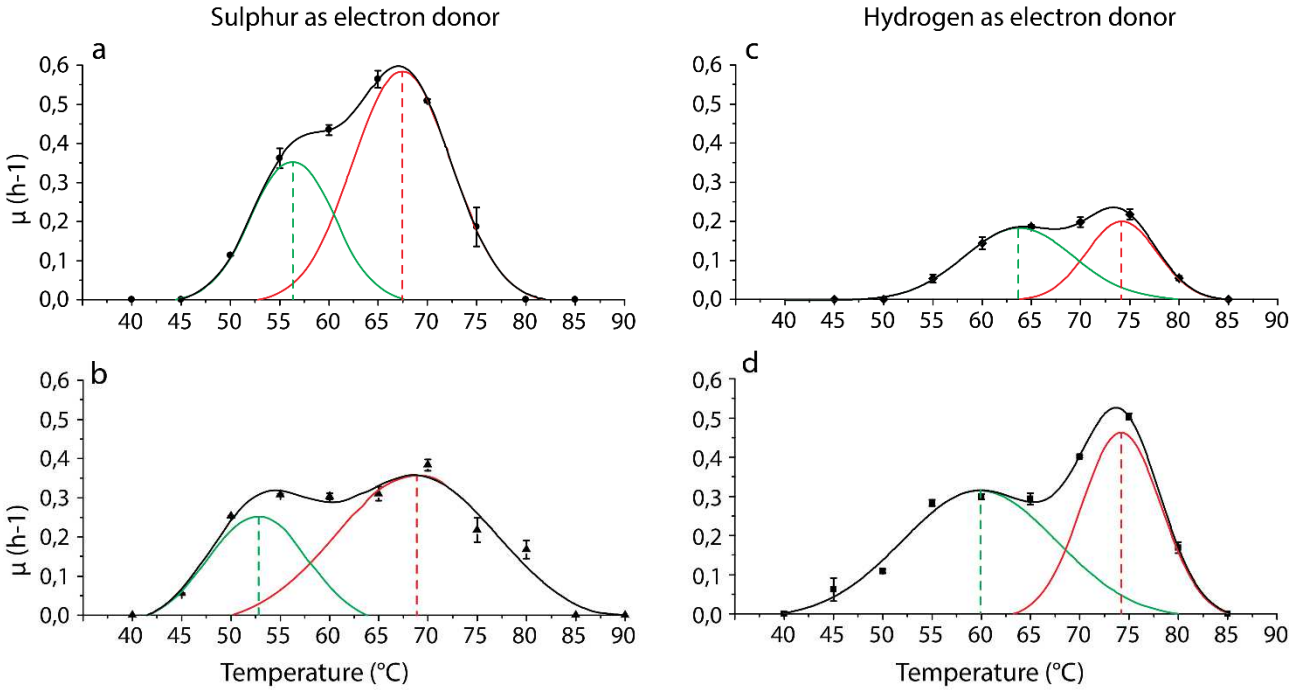

Figure 2. Effect of temperature (°C) on the specific growth rate (h $^{-1}$) of *Persephonella atlantica* strain MO1340^T. Cells were grown on (a) S^0/O_2; (b) $S_2O_3^{2-}/O_2$; (c) H_2/O_2; (d) H_2/NO_3^-. Black lines correspond to experimental curves. Green and red lines correspond to bimodal fitted curves. Standard errors based on triplicate experiments are shown for each condition.

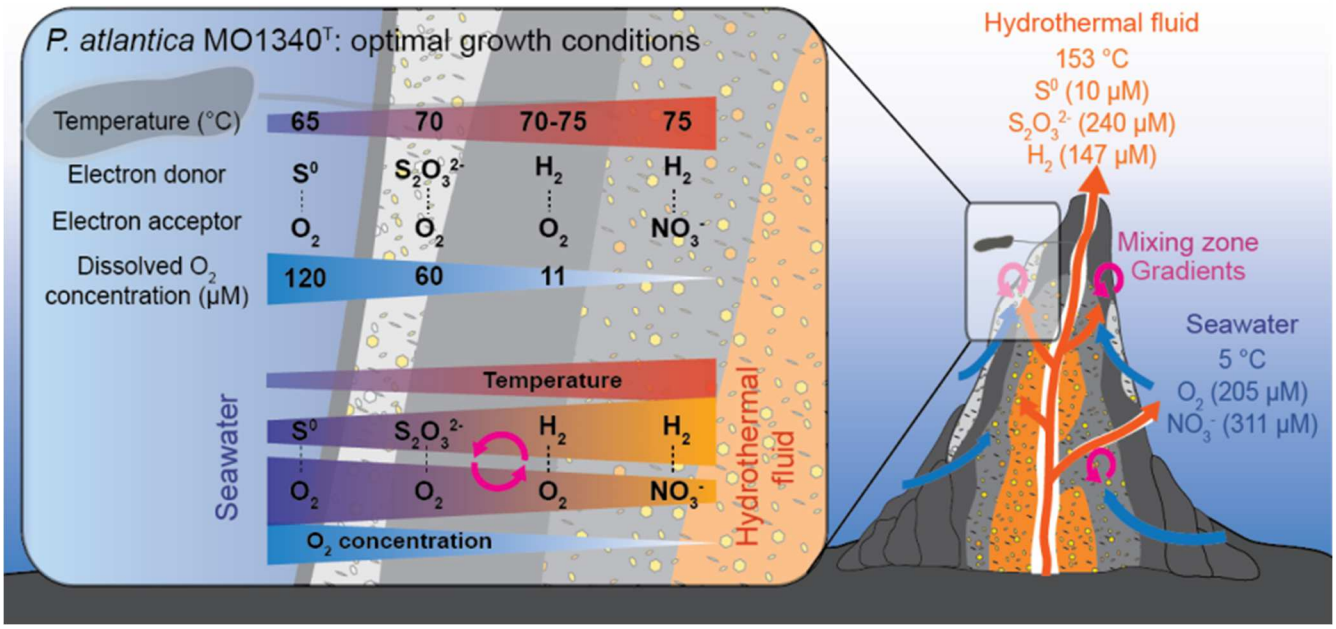

Figure 3. Schematic comparison of optimal temperatures and O_2 concentrations for *Persephonella atlantica* strain MO1340^T depending on catabolic substrates and *in situ* thermal and chemical gradients observed during the mixing of hydrothermal fluid and seawater. Concentration of chemicals species correspond to the maximal concentrations measured *in situ* or calculated for the hydrothermal physico-chemical gradient between 5 and 153 °C (details in section *Thermodynamic calculations and Arrhenius parameters*).

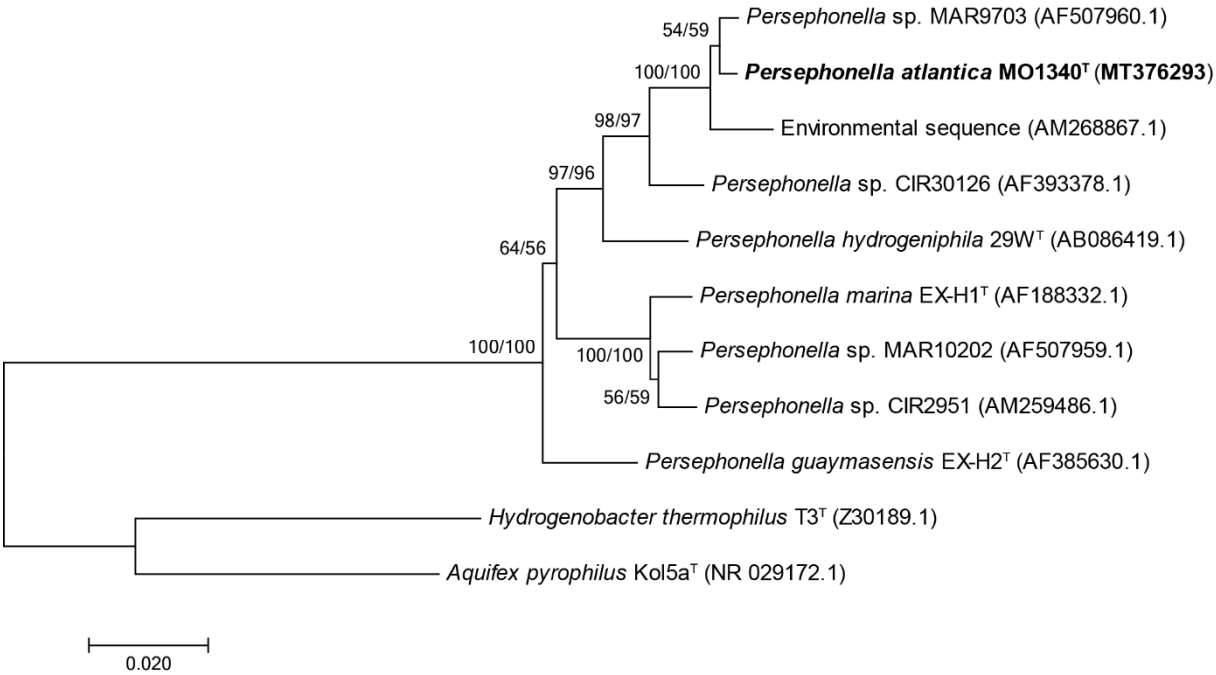

Figure 4. Phylogenetic tree of members of order *Aquificales* based on 16S rRNA gene sequences (1364 bp) showing the position of *Persephonella atlantica* strain MO1340^T among related species. Trees reconstructed using the neighbour-joining (NJ) and maximum-likelihood (ML) methods displayed the same topology. Bootstrap values (shown in the order

NJ/ML) are given to the left of each node. Bar represents 0.02 changes per nucleotide position. Numbers in parentheses are GenBank/EMBL/DDBJ accession numbers.

Table 1. Comparison of some characteristics of strain MO1340^T with other closest marine strains within the family *Hydrogenothermaceae.* Strain MO1340^T (this study); *Persephonella hydrogeniphila* 29W^T [50]; *P. marina* EX-H1^T [25]; *P. guaymasensis* EX-H2^T [25]; *Hydrogenothermus marinus* VM1^T [72]; +, positive; -, negative; *, only with O_2 as electron acceptor; **, shown in this study; [a], culture grown with S^0/O_2; [b], culture grown with $S_2O_3^{2-}/O_2$; [c], culture grown with H_2/O_2 ; [d], culture grown with H_2/NO_3; ¤ Inconsistent growth; ND, not determined. Oxygen concentration presented was calculated in gas phase. DNA G+C content was calculated from genome analysis.

Characteristics	Strain MO1340	*P. hydrogeniphila* 29W^T	*P. marina* EX-H1^T	*P. guaymasensis* EX-H2^T	*Hydrogenothermus marinus* VM1^T
Cell morphology	rods	rods - cocci	rods	rods	rods
Cell size (length/width µm)	1.4-2.2 / 0.5-0.8	2.3-2.7 / 0.9-1	2-4 / 0.3-0.4	2-4 / 0.3-0.4	2-4 / 1-1.5
Motility	+	+	+	+	+
Temperature range	50-75[a] ; 45-80[bd] ; 55-80[c]	50-72.5[d]	55-90[d]	60-80[d]	65[c]
Temperature optimum (°C)	65[a] ; 70[b] ; 70-75[c] ; 75[d]	70[d]	70[d]	75[d]	45-80[c]
pH optimum	6.5[b]	7.2[d]	6[d]	6[d]	5-7[c]
pH range	5.30 - 7[b]	5.5-7.6[d]	4.7-7.5[d]	4.7-7.5[d]	5-7[c]
NaCl optimum (% w/v)	2.5[b]	2.5[d]	2.5[d]	2.5[d]	2-3[c]
NaCl range (% w/v)	1.5-3.5[b]	1.5-5.0[d]	1.0-4.5[d]	1.0-4.5[d]	0.5-6[c]
O2 optimum (mM)	7.36[a] ; 3.68[b] ; 0.7[c]	0.63-0.84[c]	0.97-1.45[c]	0.97-1.45[c]	0.69-1.38[c]
O2 range (mM)	0.52-> 11[a] ; 0,52-10.5[b] ; ND-3.5[c]	0.10-1.05[c]	ND-< 4.53[c]	ND-< 5.32[c]	0.34-5.53[c]
Electron donors	H_2, $S_2O_3^{2-}$ *, S^0*	H_2, $S_2O_3^{2-}$**	H_2, $S_2O_3^{2-}$*, S^0*	H_2, $S_2O_3^{2-}$*, S^0*	H_2
Electron acceptors	NO_3^-, O_2	NO_3^-, O_2	NO_3^-, O_2, S^0, SO_4^{2-} ¤, acetate ¤	NO_3^-, O_2	O_2
Genome accession number	JAACYA000000000	NZ_OBEI00000000	NC_012440	-	NZ_REFO00000000
G + C content (mol%)	37.1	35.1	37.1	-	27.7
Size (Mb)	1.89	2.0	1.98	-	1.60
No. of contigs	5	19	2	-	19
No. of ORFs	2028	2130	2083	-	1713

Table 2. Summary of catabolic reactions performed by *Persephonella atlantica* strain MO1340^T and physiological parameters according to substrates couples. ¤ Optimal temperature corresponding to the two peaks observed by bimodal Gauss fitting of growth curves reported in figure 3. Putative *in situ* ΔGr values at 72 °C were calculated at optimal growth temperature of the reactions, using the high concentration range from Rommeveaux *et al* [61].

Reaction	Optimal growth temperature (range) °C	1st and 2nd peak from bimodal fitted curves (°C) ¤	Optimal O_2 concentration in gas phase (range) mM	Optimal dissolved O_2 concentration (range) µM	Q_{10} (range of linearity on Arrhenius plot, °C)	ΔGr (kJ/mol)
$S^0 + 1.5\ O_2 + H_2O \rightarrow SO_4^{2-} + 2\ H^+$	65 (55-80)	56.3-67.4	7.36 (0.52-> 11)	119.7 (8.5-> 179.5)	1,53 (55-65)	-517
$S_2O_3^{2-} + 2\ O_2 + H_2O \rightarrow 2\ SO_4^{2-} + 2\ H^+$	70 (45-80)	52.7-68.8	3.68 (0.52-10.5)	59.8 (8.5-170.9)	1,18 (50-70)	-731
$2\ H_2 + O_2 + \rightarrow 2\ H_2O$	70-75 (55-80)	63.7-74.1	0.7 (ND-< 3.5)	11.4 (ND-< 57)	1,3 (60-75)	-280
$2.5\ H_2 + NO_3^- + H^+ \rightarrow 0.5\ N_2 + 3\ H_2O$	75 (45-80)	59.8-74.2	ND	ND	1,33 (55-75)	-271

538 Table 3. Description of *Persephonella atlantica* sp. nov.

Genus name	*Persephonella*
Species name	*Persephonella atlantica*
Specific epithet	*atlantica*
Species status	sp. nov.
Species etymology	at.lan'ti.ca. L. fem. adj. atlantica for being isolated from the Atlantic Ocean
Description of the new taxon and diagnostic traits	Gram-negative cells, motile short rods with a mean length of 1.4-2.2 µm and a width of 0.5-0.8 µm. Colonies are orange, round and regular with a diameter of 1 mm. Strict chemolithoautotroph growing in microaerophilic or anaerobic conditions. No heterotophic or mixotrophic growth was observed. Vitamins or organic chelators are not necessary for growth. Uses hydrogen, thiosulphate or elemental sulphur with oxygen as electron acceptor. Sulphate is produced from oxidation of sulphur compounds. Hydrogen can also be coupled to nitrate reduction, producing nitrogen. Growth was observed for strain MO1340^T at NaCl concentrations ranging from 1.5 to 4.5 % (w/v) with an optimum at 2.5 % and at pH between 5.3 and 7.0 with an optimum around 6.5. Optimal growth temperature is respectively 65, 70, 70-75 and 75 °C, and optimal dissolved oxygen concentration is 119.7, 59.8, 11.4 and <0.2 µM for the following redox couples: S^0/O_2, $S_2O_3^{2-}/O_2$, H_2/O_2, H_2/NO_3^-.
Country of origin	EEZ Portugal
Region of origin	Lucky Strike hydrothermal field
Date of isolation (dd/mm/yyyy)	29/01/2018
Source of isolation	Black smoker chimney
Sampling date (dd/mm/yyyy)	12/08/2008
Latitude (xx°xx′xx″N/S)	37° 17' 20.26" N
Longitude (xx°xx′xx″E/W)	32° 16' 32.05" W
16S rRNA gene accession nr.	MT376293
Genome accession number	JAACYA000000000
Genome status	Incomplete (5 contigs > 500 bp)
Genome size	1.892.283 bp
GC mol%	37.07
Number of strains in study	1
Information related to the Nagoya Protocol	MOMAR 2008 oceanographic cruise. Nota verbal n°2406 June 02 2008 from ministerio dos négocios estrangeiros Portugal
Designation of the Type Strain	MO1340^T
Strain Collection Numbers	UBOCC-M-3359 = JCM 34026

References

[1] Amend, J.P., McCollom, T.M., Hentscher, M., Bach, W. (2011) Catabolic and anabolic energy for chemolithoautotrophs in deep-sea hydrothermal systems hosted in different rock types. Geochim. Cosmochim. Acta. 75, 5736-5748.

[2] Amend, J.P., Shock, E.L. (2001) Energetics of overall metabolic reactions of thermophilic and hyperthermophilic Archaea and Bacteria. FEMS Microbiol. Rev. 25, 175-243.

[3] Bankevich, A., Nurk, S., Antipov, D., Gurevich, A.A., Dvorkin, M., Kulikov, A.S., Lesin, V.M., Nikolenko, S.I., Pham, S., Prjibelski, A.D. (2012) SPAdes: a new genome assembly algorithm and its applications to single-cell sequencing. J. Comput. Biol. 19, 455-477.

[4] Berg, I.A. (2011) Ecological aspects of the distribution of different autotrophic CO_2 fixation pathways. Appl. Environ. Microbiol. 77, 1925-1936.

[5] Campbell, B.J., Engel, A.S., Porter, M.L., Takai, K. (2006) The versatile ε-proteobacteria: key players in sulphidic habitats. Nat. Rev. Microbiol. 4, 458.

[6] Chavagnac, V., Ali, H.S., Jeandel, C., Leleu, T., Destrigneville, C., Castillo, A., Cotte, L., Waeles, M., Cathalot, C., Laes-Huon, A. (2018) Sulfate minerals control dissolved rare earth element flux and Nd isotope signature of buoyant hydrothermal plume (EMSO-Azores, 37° N Mid-Atlantic Ridge). Chem. Geol. 499, 111-125.

[7] Chun, J., Oren, A., Ventosa, A., Christensen, H., Arahal, D.R., da Costa, M.S., Rooney, A.P., Yi, H., Xu, X.-W., De Meyer, S. (2018) Proposed minimal standards for the use of genome data for the taxonomy of prokaryotes. Int. J. Syst. Evol. Microbiol. 68, 461-466.

[8] Cotte, L., Waeles, M., Pernet-Coudrier, B., Sarradin, P.-M., Cathalot, C., Riso, R.D. (2015) A comparison of in situ vs. ex situ filtration methods on the assessment of dissolved and particulate metals at hydrothermal vents. Deep Sea Res. (I Oceanogr. Res. Pap.). 105, 186-194.

[9] Crozier, T.E., Yamamoto, S. (1974) Solubility of hydrogen in water, sea water, and sodium chloride solutions. J. Chem. Eng. Data. 19, 242-244.

[10] Dahle, H., Bauer, S.L.M., Baumberger, T., Stokke, R., Pedersen, R.B., Thorseth, I.H., Steen, I.H. (2018) Energy landscapes in hydrothermal chimneys shape distributions of primary producers. Front. Microbiol. 9, 1570.

[11] Dick, G.J. (2019) The microbiomes of deep-sea hydrothermal vents: distributed globally, shaped locally. Nat. Rev. Microbiol. 1.

[12] Dick, J.M. (2019) CHNOSZ: Thermodynamic calculations and diagrams for geochemistry. Front. Earth Sci. 7, 180.

[13] Eden, P.A., Schmidt, T.M., Blakemore, R.P., Pace, N.R. (1991) Phylogenetic analysis of *Aquaspirillum magnetotacticum* using polymerase chain reaction-amplified 16S rRNA-specific DNA. Int. J. Syst. Evol. Microbiol. 41, 324-325.

[14] Eder, W., Huber, R. (2002) New isolates and physiological properties of the *Aquificales* and description of *Thermocrinis albus* sp. nov. Extremophiles. 6, 309-318.

[15] Edgar, R.C. (2004) MUSCLE: multiple sequence alignment with high accuracy and high throughput. Nucleic Acids Res. 32, 1792-1797.

[16] Escartin, J. (2008) MoMAR'08–Leg 1 (Lucky Strike). Cruise Report. 9-24 Aug 2008. N/O Atalante–Victor 6000. doi 10.17600/8010110.

[17] Felsenstein, J. (1985) Confidence limits on phylogenies: an approach using the bootstrap. Evolution. 783-791.

[18] Ferrera, I., Banta, A.B., Reysenbach, A.-L. (2014) Spatial patterns of *Aquificales* in deep-sea vents along the Eastern Lau Spreading Center (SW Pacific). Syst. Appl. Microbiol. 37, 442-448.

[19] Findlay, A.J., Estes, E.R., Gartman, A., Yücel, M., Kamyshny, A., Luther, G.W. (2019) Iron and sulfide nanoparticle formation and transport in nascent hydrothermal vent plumes. Nat. Commun. 10, 1-7.
[20] Foustoukos, D.I., Houghton, J.L., Seyfried Jr, W.E., Sievert, S.M., Cody, G.D. (2011) Kinetics of H_2–O_2–H_2O redox equilibria and formation of metastable H2O2 under low temperature hydrothermal conditions. Geochim. Cosmochim. Acta. 75, 1594-1607.
[21] Friedrich, C.G., Bardischewsky, F., Rother, D., Quentmeier, A., Fischer, J. (2005) Prokaryotic sulfur oxidation. Curr. Opin. Microbiol. 8, 253-259.
[22] Friedrich, C.G., Rother, D., Bardischewsky, F., Quentmeier, A., Fischer, J. (2001) Oxidation of reduced inorganic sulfur compounds by bacteria: emergence of a common mechanism? Appl. Environ. Microbiol. 67, 2873-2882.
[23] Frigaard, N.-U., Dahl, C. (2008) Sulfur metabolism in phototrophic sulfur bacteria. Adv. Microb. Physiol. 54, 103-200.
[24] Goris, J., Konstantinidis, K.T., Klappenbach, J.A., Coenye, T., Vandamme, P., Tiedje, J.M. (2007) DNA–DNA hybridization values and their relationship to whole-genome sequence similarities. Int. J. Syst. Evol. Microbiol. 57, 81-91.
[25] Götz, D., Banta, A., Beveridge, T., Rushdi, A., Simoneit, B., Reysenbach, A. (2002) Persephonella marina gen. nov., sp. nov. and *Persephonella guaymasensis* sp. nov., two novel, thermophilic, hydrogen-oxidizing microaerophiles from deep-sea hydrothermal vents. Int. J. Syst. Evol. Microbiol. 52, 1349-1359.
[26] Guillou, C., Guespin-Michel, J. (1996) Evidence for two domains of growth temperature for the psychrotrophic bacterium *Pseudomonas fluorescens* MF0. Appl. Environ. Microbiol. 62, 3319-3324.
[27] Guiral, M., Prunetti, L., Aussignargues, C., Ciaccafava, A., Infossi, P., Ilbert, M., Lojou, E., Giudici-Orticoni, M.-T., The hyperthermophilic bacterium Aquifex aeolicus: from respiratory pathways to extremely resistant enzymes and biotechnological applications, in: Adv. Microb. Physiol., Elsevier, 2012, pp. 125-194.
[28] Gupta, R.S., The Phylum Aquificae, in: The Prokaryotes, Springer, Berlin, Heidelberg, 2014, pp. 417-445.
[29] Gupta, R.S., Lali, R. (2013) Molecular signatures for the phylum Aquificae and its different clades: proposal for division of the phylum Aquificae into the emended order *Aquificales*, containing the families *Aquificaceae* and *Hydrogenothermaceae*, and a new order *Desulfurobacteriales* ord. nov., containing the family *Desulfurobacteriaceae*. Antonie Van Leeuwenhoek. 104, 349-368.
[30] Gurevich, A., Saveliev, V., Vyahhi, N., Tesler, G. (2013) QUAST: quality assessment tool for genome assemblies. Bioinformatics. 29, 1072-1075.
[31] Hannington, M.D., Jonasson, I.R., Herzig, P.M., Petersen, S. (1995) Physical and chemical processes of seafloor mineralization at mid-ocean ridges. Geoph. Monog. Ame. Geoph. Un. 91, 115-115.
[32] Hügler, M., Huber, H., Molyneaux, S.J., Vetriani, C., Sievert, S.M. (2007) Autotrophic CO_2 fixation via the reductive tricarboxylic acid cycle in different lineages within the phylum Aquificae: evidence for two ways of citrate cleavage. Environ. Microbiol. 9, 81-92.
[33] Hügler, M., Sievert, S.M. (2011) Beyond the Calvin cycle: autotrophic carbon fixation in the ocean. Annu. Rev. Mar. Sci. 3, 261-289.
[34] Janecky, D., Seyfried Jr, W. (1984) Formation of massive sulfide deposits on oceanic ridge crests: Incremental reaction models for mixing between hydrothermal solutions and seawater. Geochim. Cosmochim. Acta. 48, 2723-2738.
[35] Kawasumi, T., Igarashi, Y., Kodama, T., Minoda, Y. (1984) Hydrogenobacter thermophilus gen. nov., sp. nov., an extremely thermophilic, aerobic, hydrogen-oxidizing bacterium. Int. J. Syst. Evol. Microbiol. 34, 5-10.

[36] Kearse, M., Moir, R., Wilson, A., Stones-Havas, S., Cheung, M., Sturrock, S., Buxton, S., Cooper, A., Markowitz, S., Duran, C. (2012) Geneious Basic: an integrated and extendable desktop software platform for the organization and analysis of sequence data. Bioinformatics. 28, 1647-1649.
[37] Kelley, D.E., Richards, C. (2015) The gsw package.
[38] Kumar, S., Stecher, G., Tamura, K. (2016) MEGA7: Molecular Evolutionary Genetics Analysis version 7.0 for bigger datasets. Mol. Biol. Evol. msw054.
[39] L'Haridon, S., Reysenbach, A.-L., Tindall, B., Schönheit, P., Banta, A., Johnsen, U., Schumann, P., Gambacorta, A., Stackebrandt, E., Jeanthon, C. (2006) *Desulfurobacterium atlanticum* sp. nov., Desulfurobacterium pacificum sp. nov. and *Thermovibrio guaymasensis* sp. nov., three thermophilic members of the Desulfurobacteriaceae fam. nov., a deep branching lineage within the Bacteria. Int. J. Syst. Evol. Microbiol. 56, 2843-2852.
[40] LaRowe, D.E., Dale, A.W., Aguilera, D.R., L'Heureux, I., Amend, J.P., Regnier, P. (2014) Modeling microbial reaction rates in a submarine hydrothermal vent chimney wall. Geochim. Cosmochim. Acta. 124, 72-97.
[41] Lin, T., Ver Eecke, H., Breves, E., Dyar, M., Jamieson, J., Hannington, M., Dahle, H., Bishop, J., Lane, M., Butterfield, D. (2016) Linkages between mineralogy, fluid chemistry, and microbial communities within hydrothermal chimneys from the Endeavour Segment, Juan de Fuca Ridge. Geom. Geophy. Geosy. 17, 300-323.
[42] Mah, R., Smith, M., Baresi, L. (1978) Studies on an acetate-fermenting strain of Methanosarcina. Appl. Environ. Microbiol. 35, 1174-1184.
[43] Mangiapia, M., Scott, K. (2016) From CO_2 to cell: energetic expense of creating biomass using the Calvin–Benson–Bassham and reductive citric acid cycles based on genome data. FEMS Microbiol. Lett. 363, fnw054.
[44] McCollom, T.M. (2000) Geochemical constraints on primary productivity in submarine hydrothermal vent plumes. Deep Sea Res. (I Oceanogr. Res. Pap.). 47, 85-101.
[45] McCollom, T.M. (2007) Geochemical constraints on sources of metabolic energy for chemolithoautotrophy in ultramafic-hosted deep-sea hydrothermal systems. Astrobiology. 7, 933-950.
[46] McCollom, T.M., Shock, E.L. (1997) Geochemical constraints on chemolithoautotrophic metabolism by microorganisms in seafloor hydrothermal systems. Geochim. Cosmochim. Acta. 61, 4375-4391.
[47] Mino, S., Maikita, H., Toki, T., Miyazaki, J., Kato, S., Watanabe, H., Imachi, H., Watsuji, T.-o., Nunoura, T., Kojima, S. (2013) Biogeography of Persephonella in deep-sea hydrothermal vents of the Western Pacific. Front. Microbiol. 4, 107.
[48] Mohr, P.W., Krawiec, S. (1980) Temperature characteristics and Arrhenius plots for nominal psychrophiles, mesophiles and thermophiles. Microbiology. 121, 311-317.
[49] Nakagawa, S., Takai, K. (2008) Deep-sea vent chemoautotrophs: diversity, biochemistry and ecological significance. FEMS Microbiol. Ecol. 65, 1-14.
[50] Nakagawa, S., Takai, K., Horikoshi, K., Sako, Y. (2003) *Persephonella hydrogeniphila* sp. nov., a novel thermophilic, hydrogen-oxidizing bacterium from a deep-sea hydrothermal vent chimney. Int. J. Syst. Evol. Microbiol. 53, 863-869.
[51] Nakagawa, S., Takai, K., Inagaki, F., Chiba, H., Ishibashi, J.-i., Kataoka, S., Hirayama, H., Nunoura, T., Horikoshi, K., Sako, Y. (2005) Variability in microbial community and venting chemistry in a sediment-hosted backarc hydrothermal system: impacts of subseafloor phase-separation. FEMS Microbiol. Ecol. 54, 141-155.
[52] Nakagawa, S., Takai, K., Inagaki, F., Hirayama, H., Nunoura, T., Horikoshi, K., Sako, Y. (2005) Distribution, phylogenetic diversity and physiological characteristics of epsilon-Proteobacteria in a deep-sea hydrothermal field. Environ. Microbiol. 7, 1619-1632.

685 [53] Nevot, M., Deroncele, V., Montes, M.J., Mercade, E. (2008) Effect of incubation
686 temperature on growth parameters of Pseudoalteromonas antarctica NF3 and its production of
687 extracellular polymeric substances. J. Appl. Microbiol. 105, 255-263.
688 [54] Parkes, R.J., Sass, H., Webster, G., Watkins, A.J., Weightman, A.J., O'Sullivan, L.A.,
689 Cragg, B.A., Methods for studying methanogens and methanogenesis in marine sediments, in:
690 Handbook of Hydrocarbon and Lipid Microbiology, Springer, 2010, pp. 3799-3826.
691 [55] Parks, D.H., Chuvochina, M., Waite, D.W., Rinke, C., Skarshewski, A., Chaumeil, P.-A.,
692 Hugenholtz, P. (2018) A standardized bacterial taxonomy based on genome phylogeny
693 substantially revises the tree of life. Nat. Biotechnol. 36, 996-1004.
694 [56] Parks, D.H., Imelfort, M., Skennerton, C.T., Hugenholtz, P., Tyson, G.W. (2015)
695 CheckM: assessing the quality of microbial genomes recovered from isolates, single cells, and
696 metagenomes. Genome Res. 25, 1043-1055.
697 [57] Ratkowsky, D., Lowry, R., McMeekin, T., Stokes, A., Chandler, R. (1983) Model for
698 bacterial culture growth rate throughout the entire biokinetic temperature range. J. Bacteriol.
699 154, 1222-1226.
700 [58] Reysenbach, A.-L., Gotz, D., Banta, A., Jeanthon, C., Fouquet, Y. (2002) Expanding the
701 distribution of the Aquificales to the deep-sea vents on Mid-Atlantic Ridge and Central Indian
702 Ridge. Cah. Biol. Mar. 43, 425-428.
703 [59] Reysenbach, A.-L., Hamamura, N., Podar, M., Griffiths, E., Ferreira, S., Hochstein, R.,
704 Heidelberg, J., Johnson, J., Mead, D., Pohorille, A. (2009) Complete and draft genome
705 sequences of six members of the Aquificales. J. Bacteriol. 191, 1992-1993.
706 [60] Reysenbach, A.-L., Shock, E. (2002) Merging genomes with geochemistry in
707 hydrothermal ecosystems. Science. 296, 1077-1082.
708 [61] Rommevaux, C., Henri, P., Degboe, J., Chavagnac, V., Lesongeur, F., Godfroy, A.,
709 Boulart, C., Destrigneville, C., Castillo, A. (2019) Prokaryote Communities at Active
710 Chimney and In Situ Colonization Devices After a Magmatic Degassing Event (37 degrees N
711 MAR, EMSO-Azores Deep-Sea Observatory). Geochemistry Geophysics Geosystems. 20,
712 3065-3089.
713 [62] Roussel, E.G., Cragg, B.A., Webster, G., Sass, H., Tang, X., Williams, A.S., Gorra, R.,
714 Weightman, A.J., Parkes, R.J. (2015) Complex coupled metabolic and prokaryotic community
715 responses to increasing temperatures in anaerobic marine sediments: critical temperatures and
716 substrate changes. FEMS Microbiol. Ecol. 91, fiv084.
717 [63] Saitou, N., Nei, M. (1987) The neighbor-joining method: a new method for
718 reconstructing phylogenetic trees. Mol. Biol. Evol. 4, 406-425.
719 [64] Sano, R., Kameya, M., Wakai, S., Arai, H., Igarashi, Y., Ishii, M., Sambongi, Y. (2010)
720 Thiosulfate oxidation by a thermo-neutrophilic hydrogen-oxidizing bacterium,
721 *Hydrogenobacter thermophilus*. Biosci., Biotechnol., Biochem. 74, 892-894.
722 [65] Sarradin, P.-M., Cannat, M. (2015) MOMARSAT2015 cruise (Lucky Strike). Cruise
723 Report. 8-29 Aug 2015. N/O Pourquoi pas?–Victor 6000. doi 10.17600/15000200.
724 [66] Shock, E.L., Holland, M.E. (2004) Geochemical energy sources that support the
725 subsurface biosphere. GMS. 144, 153-165.
726 [67] Sievert, S.M., Hügler, M., Taylor, C.D., Wirsen, C.O., Sulfur oxidation at deep-sea
727 hydrothermal vents, in: Microbial Sulfur Metabolism, Springer, 2008, pp. 238-258.
728 [68] Sievert, S.M., Vetriani, C. (2012) Chemoautotrophy at deep-sea vents: past, present, and
729 future. Oceanography. 25, 218-233.
730 [69] Soetaert, K., Meysman, F. (2012) R-package ReacTran: Reactive Transport Modelling in
731 R. Environ. Model. Softw. 32, 49-60.
732 [70] Soetaert, K., Petzoldt, T., Meysman, F., Marelac: Tools for aquatic sciences, in, Citeseer,
733 2010.

[71] Srinivasan, V., Morowitz, H.J., Huber, H. (2012) What is an autotroph? Arch. Microbiol. 194, 135-140.
[72] Stohr, R., Waberski, A., Völker, H., Tindall, B.J., Thomm, M. (2001) *Hydrogenothermus marinus* gen. nov., sp. nov., a novel thermophilic hydrogen-oxidizing bacterium, recognition of *Calderobacterium hydrogenophilum* as a member of the genus Hydrogenobacter and proposal of the reclassification of *Hydrogenobacter acidophilus* as *Hydrogenobaculum acidophilum* gen. nov., comb. nov., in the phylum'Hydrogenobacter/Aquifex'. Int. J. Syst. Evol. Microbiol. 51, 1853-1862.
[73] Suzuki, M., Hirai, T., Arai, H., Ishii, M., Igarashi, Y. (2006) Purification, characterization, and gene cloning of thermophilic cytochrome cd1 nitrite reductase from *Hydrogenobacter thermophilus* TK-6. J. Biosci. Bioeng. 101, 391-397.
[74] Takai, K., Komatsu, T., Inagaki, F., Horikoshi, K. (2001) Distribution of archaea in a black smoker chimney structure. Appl. Environ. Microbiol. 67, 3618-3629.
[75] Tamura, K., Nei, M. (1993) Estimation of the number of nucleotide substitutions in the control region of mitochondrial DNA in humans and chimpanzees. Mol. Biol. Evol. 10, 512-526.
[76] Tatusova, T., DiCuccio, M., Badretdin, A., Chetvernin, V., Nawrocki, E.P., Zaslavsky, L., Lomsadze, A., Pruitt, K.D., Borodovsky, M., Ostell, J. (2016) NCBI prokaryotic genome annotation pipeline. Nucleic Acids Res. 44, 6614-6624.
[77] Team, R., R: A language and environment for statistical computing, in, Vienna, Austria, 2013.
[78] Thauer, R.K., Jungermann, K., Decker, K. (1977) Energy conservation in chemotrophic anaerobic bacteria. Bacteriol. Rev. 41, 100.
[79] Vuillemin, R., Le Roux, D., Dorval, P., Bucas, K., Sudreau, J., Hamon, M., Le Gall, C., Sarradin, P. (2009) CHEMINI: A new in situ CHEmical MINIaturized analyzer. Deep Sea Res. (I Oceanogr. Res. Pap.). 56, 1391-1399.
[80] Webster, G., Rinna, J., Roussel, E.G., Fry, J.C., Weightman, A.J., Parkes, R.J. (2010) Prokaryotic functional diversity in different biogeochemical depth zones in tidal sediments of the Severn Estuary, UK, revealed by stable-isotope probing. FEMS Microbiol. Ecol. 72, 179-197.
[81] Weiss, R.F., The solubility of nitrogen, oxygen and argon in water and seawater, in: Deep Sea Research and Oceanographic Abstracts, Elsevier, 1970, pp. 721-735.
[82] Wery, N., Lesongeur, F., Pignet, P., Derennes, V., Cambon-Bonavita, M.-A., Godfroy, A., Barbier, G. (2001) *Marinitoga camini* gen. nov., sp. nov., a rod-shaped bacterium belonging to the order Thermotogales, isolated from a deep-sea hydrothermal vent. Int. J. Syst. Evol. Microbiol. 51, 495-504.
[83] Wiegel, J. (1990) Temperature spans for growth: hypothesis and discussion. FEMS Microbiol. Rev. 6, 155-169.
[84] Wiegel, J., Ljungdahl, L., Rawson, J. (1979) Isolation from soil and properties of the extreme thermophile *Clostridium thermohydrosulfuricum*. J. Bacteriol. 139, 800-810.
[85] Wiegel, J., Michael, A.W., Thermophiles: The Keys to the Molecular Evolution and the Origin of Life?, CRC Press, 1998.
[86] Yang, C.-L., Chen, X.-K., Wang, R., Lin, J.-Q., Liu, X.-M., Pang, X., Zhang, C.-J., Lin, J.-Q., Chen, L.-X. (2019) Essential role of σ factor RpoF in flagellar biosynthesis and flagella-mediated motility of *Acidithiobacillus caldus*. Front. Microbiol. 10, 1130.
[87] Yoon, S.-H., Ha, S.-m., Lim, J., Kwon, S., Chun, J. (2017) A large-scale evaluation of algorithms to calculate average nucleotide identity. Antonie van Leeuwenhoek. 110, 1281-1286.

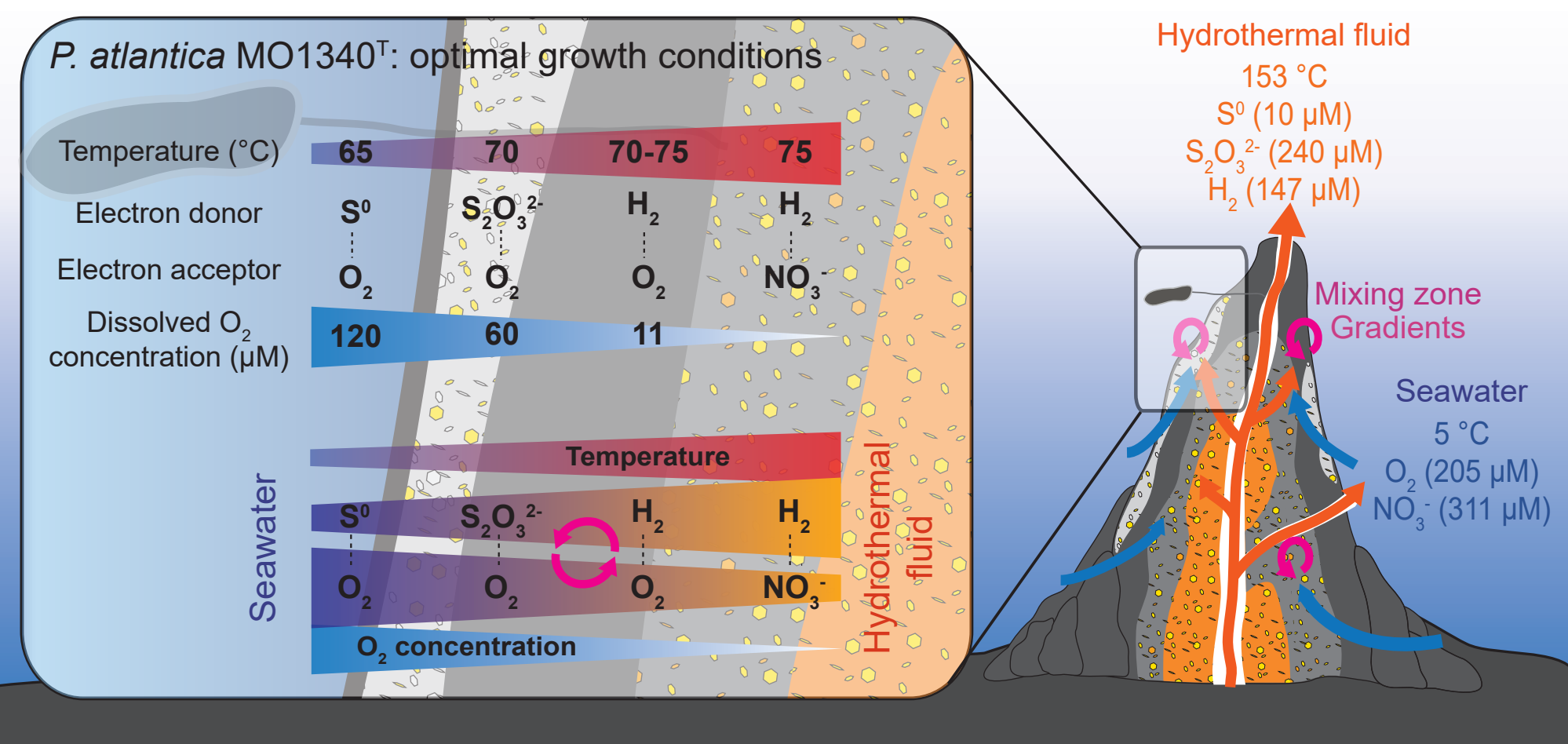
P. atlantica MO1340T: optimal growth conditions
Temperature (°C)
65
70
70-75
75
Electron donor
S0
S2O3 2-
H2
H2
Electron acceptor
O2
O2
O2
NO3 -
Dissolved O2 concentration (µM)
120
60
11
Seawater
Temperature
S0
S2O3 2-
H2
H2
O2
O2
O2
NO3 -
O2 concentration
Hydrothermal fluid
Hydrothermal fluid
153 °C
S0 (10 µM)
S2O3 2- (240 µM)
H2 (147 µM)
Mixing zone
Gradients
Seawater
5 °C
O2 (205 µM)
NO3 - (311 µM)